Proceedings of ICMM2005
3rd International Conference on Microchannels and Minichannels
June 13-15, 2005, Toronto, Ontario, Canada

ICMM2005-75206

OPTOFLUIDIC MICROSCOPY

Xin Heng[1], David Erickson[1,2], Demetri Psaltis[1], Changhuei Yang[1]

[1]Electrical Engineering, Moore Lab 136-93, California Institute of Technology, Pasadena, CA 91125
Tel (626) 395-4711, Fax (626-395-8952)
[2]Mechanical and Aerospace Engineering, Cornell University, Ithaca, NY

Email: xin@caltech.edu (X. Heng), de54@cornell.edu (D. Erickson), psaltis@sunoptics.caltech.edu (D. Psaltis), chyang@caltech.edu (C. Yang)

ABSTRACT

Recent advances in the development of lab-on-a-chip devices have been rapid and broad ranging. In general however these devices, while containing micro- or even nano-scale components, rely heavily on macroscale infrastructure (*e.g.* microscopes, chip readers and power sources) to perform much of the actual product detection and subsequent analysis. As such to enable the next generation of portable lab-on-chip devices, techniques for simply and cheaply integrating on-chip analysis functionalities will be required. In this work we present our work directed towards the development of a new concept in rapid on-chip imaging which we refer to as "optofluidic microscopy (OFM)". Here we present an overview of the imaging theory, fabrication procedure and operational details of the initial prototype. Preliminary experimental results of this on-chip optical imager are also reported. A significant advantage of the technique is that through proper spatial scaling, sub-wavelength resolution can be achieved without bulk optics.

INTRODUCTION

The development of micro-optical devices has been a very active field over the past few years due to the broad range of applications in the communications, optical analysis and displays fields. The parallel advancements in micro- and nano-scale fluidic devices control have enabled a new class of tunable micro-optical devices which collectively can be thought of as "Optofluidic" structures. Examples of such devices include planar microlenses [1], total-internal-reflection-based biochip with micromirrors [2], microfluidic lasers [3], as well as on-chip microspectrometers [4].

The past few years have seen rapid advancements in the field of microfluidics most notably the development of large-scale integration of microfluidic circuits [5], and numerous applications of microfluidics to life science research [6]. Optical microscopy is presently employed in microfluidic research as a technique to study fundamental microscale flow physics as well as biological targets and processes conducted within these integrated microfluidic systems. In general these devices relies on macro-scale infrastructure (*e.g.* bulk microscopes, chip readers) to perform the actual product analysis. On-chip optical imaging techniques which can provide much the same or better functionality of these bulk devices will thus form a critical part of next generation, portable microfluidic chips.

Here, we introduce a new technique and initial prototype for an on-chip optical imaging device which we refer to as an Optofluidic Microscope (OFM). The OFM in principle could serve to eliminate the dependence on objective lenses and complex microscope setups to obtain biological images in microscale devices, thereby enhancing their portability and compactness. In our initial prototype soft lithography pattered microfluidic system is used to transport biological targets to the detection region via either electrokinetics or pressure driven flow. In the detection region, a micron-scale hole-array is defined by electron beam lithography. The light transmission through each hole is modulated with

time by the transmission properties of the targets when they pass through the detection region. As will be discussed the image of the targets can be reconstructed through the time trace of the transmitted intensity. In the following sections we explain in more details the operational principle and theory behind the imaging technique and later we present an initial prototype and experimental results. Potential applications of this OFM device will be further discussed.

CHIP DESIGN AND FABRICATION

Figure 1(a) shows an overview of the initial prototype optofluidic microscopy chip. In this variation, biological or non-biological samples are transported to the imager using a standard microfluidic focusing arrangement defined in a poly-(dimethylsiloxane) (PDMS) based upper layer that is manufactured and designed using standard rapid prototyping/soft lithography protocols. The imager consists of an angled a micro- or nano-hole array defined in a nontransparent gold layer deposited on an optically transparent surface. Fabrication of the imaging array schematically shown in Figure 2 begins by first evaporating a layer of gold (approximately 100nm thick) on the transparent surface (in this case glass). A poly-(methylmethacrylate) (PMMA) resist layer is then spun on the gold layer and standard electron-beam lithography is used to write the hole pattern in the PMMA resist. After developing, the gold layer is wet etched thereby defining the imager holes. The remaining PMMA layer is then stripped and replaced with a new PMMA film (approximately 200nm thick) which serves to electrically isolate the gold layer from the fluidic layer. In the final assembly stage access holes are punched in the PDMS layer which is then exposed to Oxygen plasma for 30 seconds. The fluidics are then aligned and brought into contact hermetically with the imaging layer. After assembly, an 80°C post bake is used to help improve the bonding strength. Figure 1(b) shows an image of the assembled chip and its inlet provides a graphical overview of the entire microfluidic chip.

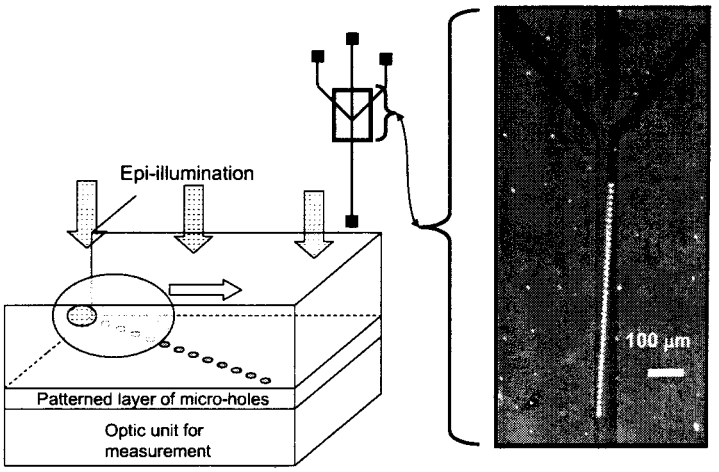

Figure 1: (a) Schematic of the OFM device. (b) Photograph of the assembled optofluidic imaging chip. In this device the channel width is approximately 44μm.

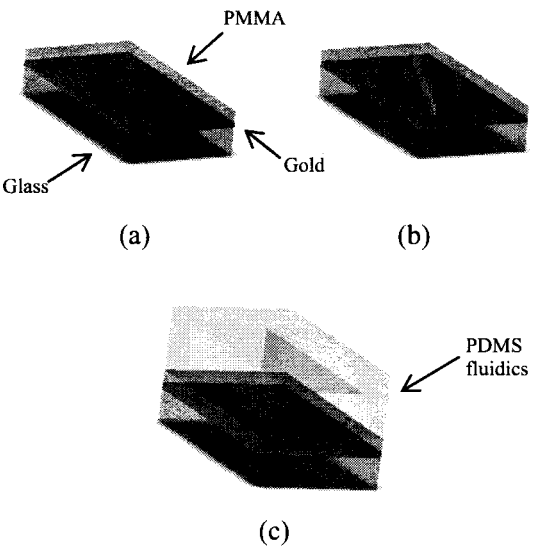

Figure 2: Schematic overview of imager fabrication and assembly procedure. (a) 100nm layer gold deposition on transparent surface followed by spin coating PMMA resist layer (b) Electron-beam lithography defines a slanted hole array in PMMA resist, develop then wet etch gold surface. (c) Remove excess PMMA and spin coat fresh 200nm layer for electrical isolation and bond with PDMS fluidics.

IMAGING METHODS AND CURRENT OPERATIONING PRINCIPAL

In the final arrangement of the OFM device, the transmission will be monitored by simply attaching a linear CCD or photodiode array directly underneath the detection layer, which will make the whole device compact and free of bulk optics. The current inter-hole

spacing of 13μm is specially designed to be the same spacing as a line scan sensor (*e.g.* Dalsa tall pixel sensor IL-C6-2048), so that the transmission through each hole will uniquely map to one single CCD pixel. In this work however, to demonstrate the optofluidic microscopy principle, we image the hole array onto a standard CCD camera mounted on an inverted microscope stand (Olympus IX-71).

The target object is made to flow through the microfluidic channel at a constant velocity using either electrokinetic control or pressure driven flow and confined to the center of the imager through upstream focusing. As shown in Figure 1(a), in the current arrangement the device is illuminated from the top. The deposited gold film on glass surface is, at 100nm, designed to be nearly opaque to white light transmission (*e.g.* the skin depth of 632.8nm He-Ne laser in a gold film is about 12nm). As the targets pass over the imaging array, the light transmission characteristics of the individual holes are modulated with time. In effect each hole functions as a pinhole in confocal microscope. The time evolution of the light power penetrating through each sub-micron hole is dependent on the spatial profile of the target as well as its optical properties. Therefore, by time tracing the transmission through each single hole, the detailed features of the target will be generated as illustrated in Figure 4 (upper).

For a flow through imager the pixel resolution in y-direction r_y, perpendicular to flow direction depends on the spacing of adjacent holes in this direction. The more holes etched through the gold layer per unit width, the higher the achievable resolution as defined by Eq. (1) below,

$$r_y = \frac{w}{n_h} \tag{1}$$

where n_h equals to the number of holes and w is the channel width. For example, in the case where the channel width is 40 μm, the y-direction pixel size would be 1 μm if there are 40 holes across the channel. In the x (flow) direction the pixel size is determined by the acquisition rate of the optical measurement unit and the net velocity of the target (i.e. the resolution in x-direction is equal to target moving speed, u, times the pixel acquisition time Δt) as defined by Eq. (2),

$$r_x = u\Delta t, \tag{2}$$

For example if the target flow speed is 100μm/s, and the detector's reading rate is 1 kHz, the maximum resolution in the x direction would be equal to 0.1micron.

The sensitivity of the OFM method depends critically on the total transmission through each hole. Assuming the metal layer is perfectly conductive, two different regimes of hole size (S_h) are examined.

$S_h >> \lambda$, Large hole limit. In this regime, the effective transmission area A_T is simply equal to the physical cross section of the hole.

$S_h << \lambda$, Small hole limit. In this regime and in the limit that the hole is infinitesimally thin, Bethe [9] showed that the effective transmission area is given is proportional to the sixth power of the pinhole diameter. In a recent work, De Abajo [10] observed that the transmission is further attenuated exponentially as a function of the hole depth. Combining these two effects, we postulate that the effective transmission area can be expressed as:

$$A_T = \left(\frac{16\pi^3}{27}\right)\left(\frac{S_h^6}{\lambda^4}\right)\exp\left(-4\pi d\sqrt{\frac{0.586^2}{S_h^2}-\frac{1}{\lambda^2}}\right) \tag{3}$$

The formulation agrees well with the simulation data that De Abajo [10] reported. The total transmission photon count for a pixel dwell time τ (also equivalent to the inverse of frame rate) is given by,

$$N_T = \frac{\varepsilon I A_T \tau}{h\frac{c}{\lambda}} \tag{4}$$

where $h\frac{c}{\lambda}$: the energy that one single photon carries; I : illumination intensity; ε : quantum efficiency of CCD camera.

The dominating noise source includes the photon

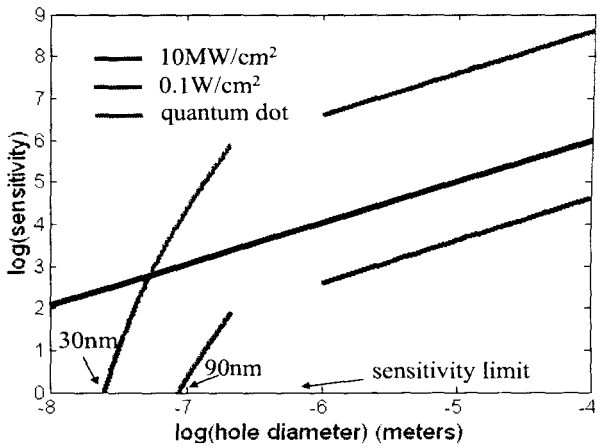

Figure 3: Transmission sensitivity curves for varying hole sizes at two illumination intensity (10MW/cm^2: biological laser illumination intensity limit, 0.1W/cm^2: ambient sunlight intensity). Green line denote the sensitivity curve for an OFM implementation with quantum dots in place of the holes (intensity ~ 100W/cm^2). This implementation is expected to perform well at high resolution. The sensitivity curves for the holes are derived through analysis in two different size regimes.

counting noise (shot noise) and the receiver noise ($n_r\tau$). Thus the sensitivity can be expressed as:

$$SNR = \frac{N_T}{\sqrt{N_T + (n_r\tau)^2}} \qquad (5)$$

Therefore, object imaging with a micron level resolution and 30dB sensitivity can be readily performed with the use of natural light illuminations. In principal sub-wavelength resolution can be achieved in an OFM device by simply spacing the adjacent holes in the y-direction at the desired resolution limit. As the holes are well separated in x-direction by 10's of microns, their transmission contributions will be distinguishable from each other on CCD camera. The state of the art nanofabrication technology enables the creation of etching patterns with resolution of 10's of nanometer. Therefore, it should be possible to create OFM devices with resolution of sub 100 nanometers. Our preliminary estimates based on Eq. (3)-(5) shown in graphical forms in Fig. 3 predicts that with 600 nm laser illumination, we can easily achieve 40 dB signal sensitivity for OFM with resolution of 100 nm.

MICROFLUIDIC TRANSPORT OF TARGETS

On the micro and nano scales, fluid flow and particulate transport can be accomplished using numerous different techniques, the most popular among which include traditional pressure driven flow, electrokinetic transport and discrete droplet translocation via electrowetting, or thermocapillarity (see Stone et al. [11] for a comprehensive overview). While imaging features created with electron beam lithography can be made as small as 10nm, the ultimate resolution of the optofluidic microscope will be limited by the vertical and horizontal confinement stability of the targets. Physical confinement requires that the channel size be on the order of that of the target being imaged, which for smaller targets (<0.5μm) could mean channel sizes on the order of 100s of nanometers. The maximum allowable pressure for use with PDMS based fluidics is on the order of 100 kPa. For a 0.5μm channel height, this implies a maximum flow rate of 70μm/s for the given pressure – a speed that is too slow for high throughput imaging purposes. Discrete droplet techniques are also not suitable as while targets could be transported over the array, without a channel structure physical confinement over the array is difficult.

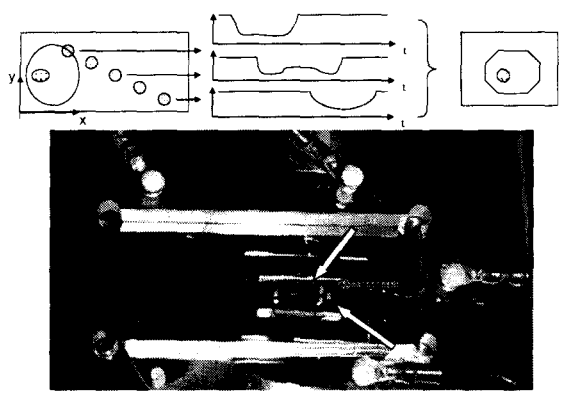

Figure 4: (upper) Operational illustration of the transmission mode optofluidic microscope; (bottom) OFM chip together with electrokinetic driving source

Electroosmotic transport results from the interaction of an externally applied electric field with the electrical double layer. The electrical double layer is a very thin region of non-zero charge density near the interface (in this case a solid-liquid interface) and is generally the result of surface adsorption of a charged species and the resulting rearrangement of the local free ions in solution so as to maintain overall electroneutrality. As it is a surface driven effect, the electrokinetic velocity is nearly independent of channel size, thus scaling much better to the physical confinement and imaging range ultimately desired here.

In addition to physical confinement, fluidic confinement of the targets will be equally important to final imaging stability. Since the pioneering works of Serge and Silberberg [12, 13] a number of researchers [*e.g.* ref. 14] have studied Brownian particle dynamics and demonstrated that particles in a shear flow tend to migrate to a particular location where the various hydrodynamic forces acting on the particle equilibrate. For pressure driven flow in low aspect ratio microchannel systems, such as those used here, there exists a strong shear gradient in the vertical direction which will tend to confine the targets at a location roughly 40% of the distance from either the upper or lower surface of the channel to the midpoint (*i.e.* there are two vertical equilibrium positions) [see Cao and Wereley, 15]. In the horizontal direction however there is no significant velocity gradient (*i.e.* in low aspect ratio channels the parabolic velocity profile in the horizontal direction tends to be very weak) and thus no mechanism to stabilize the targets against Brownian diffusion after it is initially focused into the channel. Recent advancements in localized modification of the electroosmotic mobility in microfluidic devices [16] could allow for velocity profile tuning in order to create a single shear equilibrium position for confinement against Brownian motion in both the vertical and horizontal directions. Such tuning is not possible with traditional pressure driven flow.

Our electrokinetic driven microfluidic setup is shown in Figure 4(bottom), in which white arrows represent the focusing beam directions and green ones represent the target flowing direction. As seen in Figure 3(bottom) and

Figure 1(b), in the initial prototype the fluid from the two side branches acts as a focusing force. The central channels contain the biological targets which are confined to the center of the imager through upstream focusing. By dynamically adjusting the voltage applied to the fluid, biological targets can be driven faster to get into the detection region but slower when they are passing the detection region for the purpose of obtaining more pixel information for horizontal direction. The gold layer is isolated from the electrical ports by a thin layer of PMMA. The PMMA layer and the PDMS channels are treated with oxygen plasma for tighter sealing and better flowing. The current setup only requires no higher than 50 V in the target transportation channels and less than 30V in the focusing channels to drive the biological targets with an appropriate speed for image acquisition.

INITIAL EXPERIMENTAL RESULTS AND CONCLUSIONS

As mentioned above and as illustrated in Figure 4 (upper), with the full information of the transmission time track, the geometrical profile and the interior structures of the imaging targets can be reconstructed. The biological target selected for our initial experiments were Chlamydomonas provided by Carolina biological supply. Chlamydomonas is a single-celled, biflagellate, green alga, roughly circular in shape and ranging in diameter from 10-20μm. It contains several species that have become popular as research tools, because it has well defined genetics that can transformed by well developed techniques. We have selected Chlamydomonas as our biological target for our initial experiments as it has more or less a regular shape suitable for flowing in micro-channels. As alluded to earlier in these initial experiments transmission changes through each hole were recorded by an 8-bit Sony XCD-X710 firewire CCD camera, mounted on Olympus IX-71 inverted microscope.

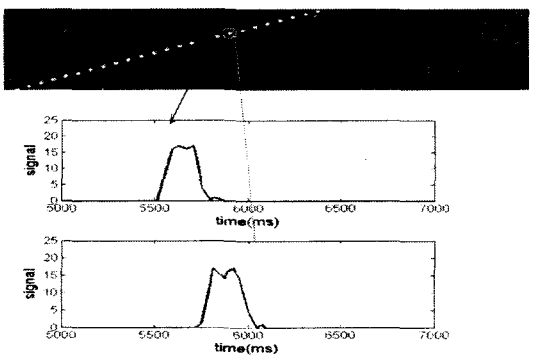

Figure 5 (upper) the change of transmission intensity through the left hole indicated by red circle and red arrow. (Bottom) the intensity change through the right hole indicated by green circle and green arrow.

Figure 5 shows the transmission change of two adjacent holes when a single Chlamydomonas cell passes over them. The continuous picture frames are streamed into a Matlab program from which the pixel information from each hole is extracted. It can be seen from the figure that the transmission through holes does respond dynamically with the object flowing across their region. With more and faster frames able to be collected, more detailed pixel information can be obtained, and the two dimensional image of the biological sample will be subsequently regenerated. The final image reconstruction is currently in progress.

This preliminary study demonstrates that the OFM imaging method is feasible and that the demonstration is readily scalable. An OFM device with sub-wavelength resolution is well within our means to fabricate. The advantages of the optofluidic microscope include high achievable resolution, low cost, compactness, small sample volume, ease of view finding and high throughput. We believe that with faster and higher resolution cameras, the more detailed structure from the biological target can be imaged; while at the same time, the ability of making nano-scale holes will push the OFM concept into the nanoscope regime, in which a lot more imaging possibilities will open up.

In addition to the above mentioned 'spatial-encoding' approach employed in our prototype OFM device, we may also use spectral encoding approaches to create another type of OFM imaging system. One such example of spectral encoding based imaging system consists of simply embedding semiconductor quantum dots with different fluorescence emission spectra in a two-dimensional hole matrix. By observing the time changing emission spectra from the matrix, we can deduce the profile of the test object that is flowing across detection matrix unit. Research into this encoding scheme is in progress.

In conclusion, we demonstrated a new type of imaging microscope that is dramatically compact (in principle, the device can be fabricated to be of the size of matchbox), is capable of high throughput processing, and is easy to implement at a mass production level. As an alternative of conventional bulky microscope, its ease of fabrication, compactness and low cost make it possess more advantages in next generation lab on a chip development. Nevertheless, the significance of OFM extends beyond simply the reasons named above. It is also a novel near field method and can potentially reach the sub wavelength resolution regime, thus opening up a new field of optical on-chi imaging of small bacteria and viruses. A high throughput approach for imaging and distinguishing different viruses or bacterium types can be very important and convenient for biological and clinical usage.

AKNOWLEDGEMENTS

This work was carried out under the funding support from the DARPA center for optofluidic integration. We thank the Caltech Watson clean room facility for the access of the micro-fabrication utility.

REFERENCES

[1] Seo J snd Lee LP, 2004, 'Disposable integrated microfluidics with self-aligned planar micro-lenses.' Sensors and actuators B-chemical 99 (2-3): 615-622;

[2] Chronis N and Lee LP, 2004, 'Total internal reflection based biochip utilizing a polymer-filled cavity with a micromirror sidewall', LAB ON A CHIP 4 (2): 125-130;

[3] Cheng, Y, Sugioka K and Midorikawa, 2004, 'Microfluidic laser imbedded in glass by three-dimensional femtosecond laser micro-processing', optics letters, 29, No.17, 2007-2009;

[4] Adams ML, Enzelberger M, Quake S, Scherer A, 2003, 'Microfluidic integration on detector arrays for absorption and fluorescence micro-spectrometers', SENSORS AND ACTUATORS A-PHYSICAL 104 (1): 25-31;

[5] Thorsen T, Maerkl SJ, Quake SR, 2002, 'Microfluidic large-scale integration', Science 298 (5593);

[6] Beebe D.J., Mensing G.A., Walker G.M., 2002, 'Physics and applications of microfluidics in biology', Annual Review of Biomedical Engineering, 261-286;

[7] Courjon D, 'Near-field microscopy and near-field optics', Imperial College Press, 2003

[8] F. de Fornel, 'Evanescent waves, from Newtonian optics and Atomic optics', Springer, 2001

[9] Bethe HA, 'Theory of diffraction by small holes', physics Review, 66, 163 (1944).

[10] F. de Abajo, 2002, 'Light transmission through a single cylindrical hole in a metallic film', *Optics Express*, vol.10, pp. 1475-1484;

[11] H.A. Stone, A.D. Stroock, A. Ajdari, 2004, "Engineering flows in small devices: Microfluidics Toward a Lab-on-a-Chip" Annu. Rev. Fluid Mech. 36, 381–411;

[12] G. Segré, A. Silberberg, 'Behavior of Macroscopic Rigid Spheres in Poiseuille Flow. Part 1', Journal of Fluid Mechanics, 14, (1962a), 115;

[13] G. Segré, A. Silberberg, "Behavior of Macroscopic Rigid Spheres in Poiseuille Flow. Part 2," J. Fluid Mech. 14, (1962a), 136;

[14] P.R. Nott, J.F. Brady, 1994, "Pressure-Driven Flow of Suspensions: Simulation and Theory," J. Fluid Mech. 275, 157.

[15] J. Cao, S. Wereley "Brownian Particle Distribution in Tube Flows" 2004 ASME International Mechanical Engineering Congress and Exposition. Anaheim, California, USA, IMECE2004-61899.

[16] E. Biddiss, D. Erickson, D. Li, 2004, "Heterogeneous surface charge enhanced micromixing for electrokinetic flows" Anal. Chem., 76, 3208;